REGIONAL CENTRE OF ADVANCED TECHNOLOGIES AND MATERIALS
Regionální centrum pokročilých technologií a materiálů

Nanotechnologies in Diagnostic and Theranostic Applications

Radek Zbořil

Regional Centre of Advanced Technologies and Materials

General Director

Palacky University in Olomouc, Czech Republic

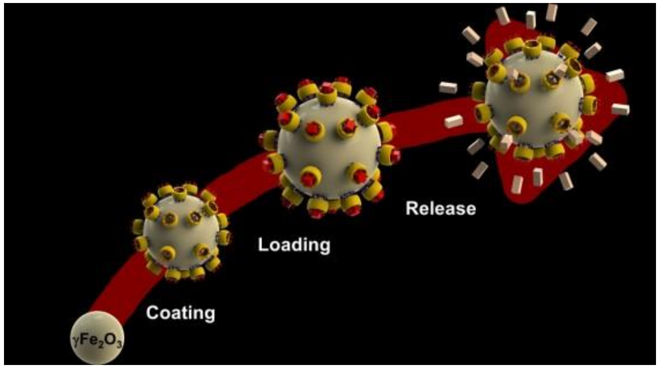

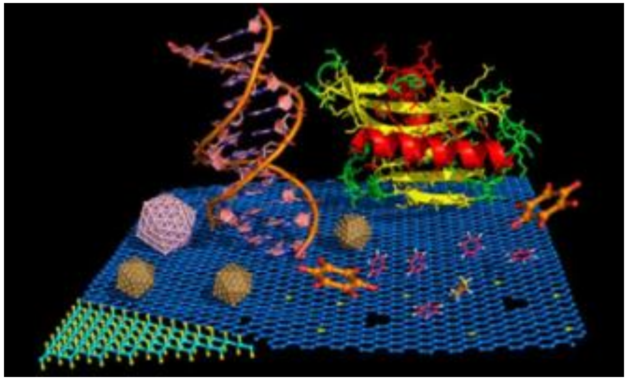

REGIONAL CENTRE OF ADVANCED TECHNOLOGIES AND MATERIALS

Regionální centrum pokročilých technologií a materiálů

REGIONAL CENTRE OF ADVANCED TECHNOLOGIES AND MATERIALS

Nanotechnologies

Chemistry, Materials Science

Optics

Environmental Technologies

Biomedicine

Computational Chemistry

140 scientists
20 countries

REGIONAL CENTRE OF ADVANCED TECHNOLOGIES AND MATERIALS

Regionální centrum pokročilých technologií a materiálů

Biomedicine

Nanosilver Based Antimicrobial Technologies

- Quantification of antibacterial and antifungal activity, toxicity
- Covalent immobilization on solid surfaces, antimicrobial coatings
- Targeted antibacterial action – magnetic nanosilver
- Synergy with ATB

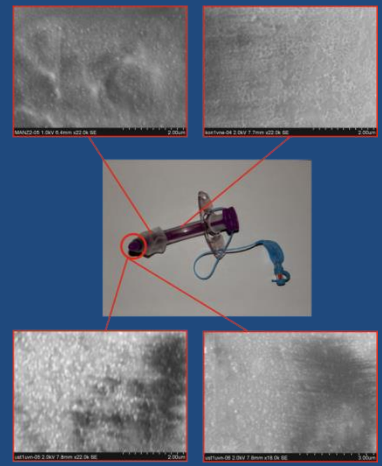

e.g. Biomaterials 32 (2011) 4704.

MRI contrast agents

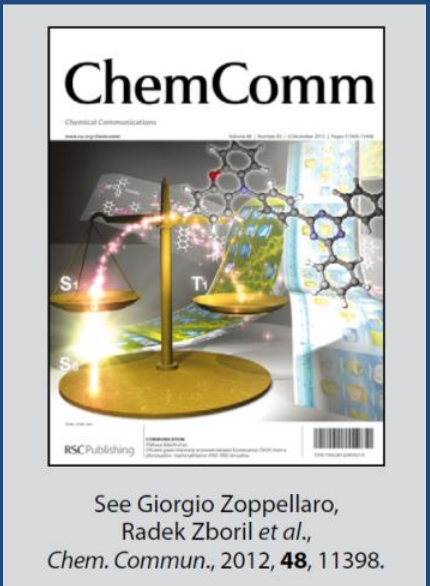

Targeted Drug Delivery & Theranostics

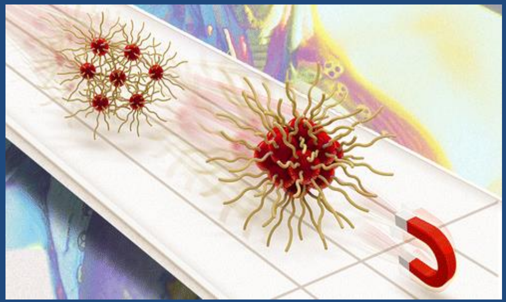

Magnetic iron oxide nanoclusters

e.g. Chem. Mater. 26 (2014) 2062.

Magnetic SERS

Magnetic nanosilver used for highly sensitive and selective determination of biosubstances (a new in vitro diagnostics)

Carbon quantum dots

Optical imaging and theranostics

Chem. Mater 24 (2012) 6.
Carbon 70 (2014) 279.

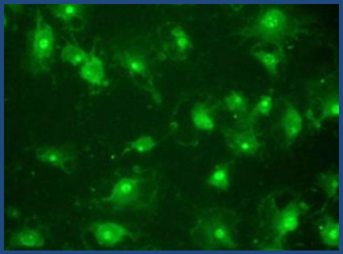

ANAL. CHEM., 86 (2014) 2939. ANAL. CHEM., 86 (2014) 11107.

NANOSILVER in ANTIMICROBIAL TREATMENT

REGIONAL CENTRE OF ADVANCED TECHNOLOGIES AND MATERIALS

Regionální centrum pokročilých technologií a materiálů

ANTIBACTERIAL & ANTIFUNGAL ACTION, FUNCTIONALIZATION

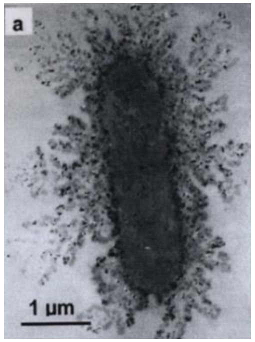

JPC-B 110 (2006) 16248. > 1000 citations

Biomaterials 30 (2009) 6333. > 300 citations

TOXICITY, SYNERGY WITH ATB, MAGNETIC TARGETING

EST 45 (2011) 4974; *EST* 47 (2013) 757.

Green Chem. 14 (2012) 2550.

Biomaterials 32 (2011) 4704. > 100 citations

JPC-C 112 (2008) 5825. > 350 citations

ANTIMICROBIAL COATINGS, IN VIVO

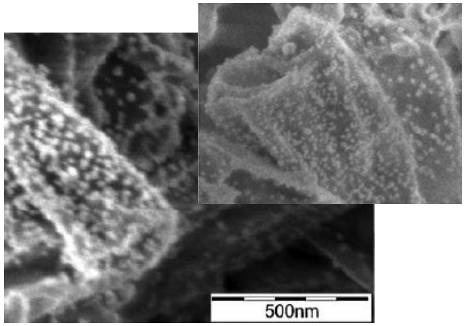

Patent No. 303502, 2012.

Today use of Ag NPs

Tracheostomy cannulas

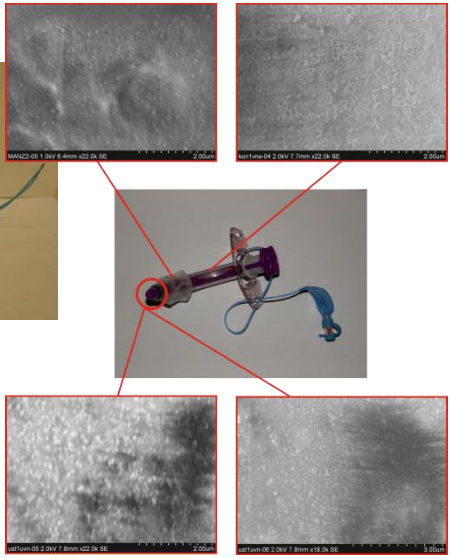

Clinical trials in Prague

Carbon based quantum dots (CDs)

REGIONAL CENTRE OF ADVANCED TECHNOLOGIES AND MATERIALS
Regionální centrum pokročilých technologií a materiálů

Properties, advantages:

- ➢ Ultrasmall particles < 10 nm
- ➢ Graphitic core with various surface functionalities (C,H,N, O nature)
- ➢ Large scale production
- ➢ Biocompatible nature, low toxicity
- ➢ Multi-colour wavelength dependent emission (size, functional groups)
- ➢ Resistance to photobleaching
- ➢ Easy to functionalize the surface (PEG..)
- ➢ Two sources of fluorescence: carbon core, organic surface layer ⇒ controllable PL properties

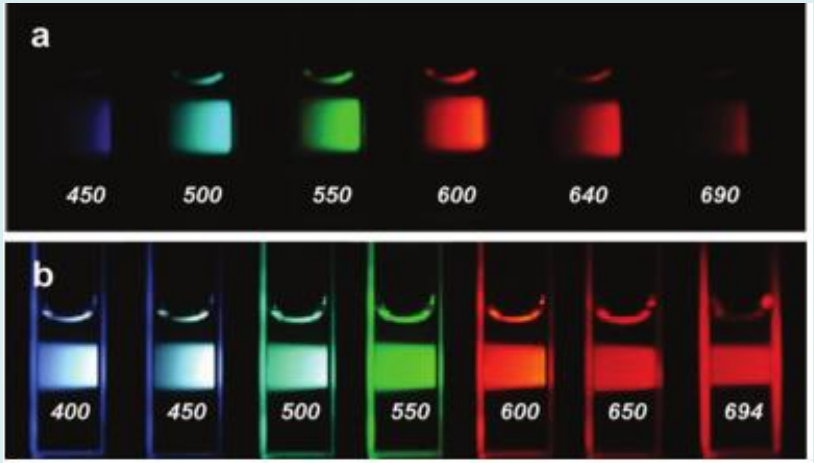

* *Chem. Mater*. 20 (2008) 4539; *Small* 4 (2008) 455; > 600 citations; *Chem. Mater 24* (2012) 6; *JACS 134 (2012) 747; Carbon 61 (2013) 640*

Selective nucleus vs cytoplasm cell labeling

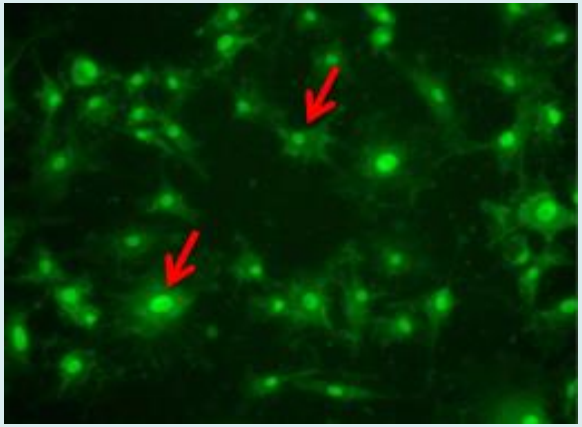

mouse fibroblast NIH/3T3 cells labeled with CDs

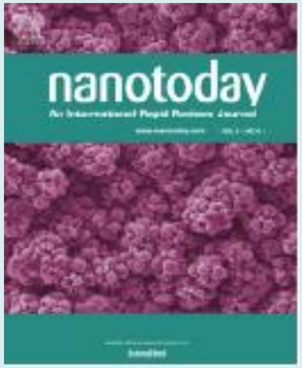

Hola et al. ***NANO TODAY*** 9 (**2014**) 590-603.

Georgakilas et al. ***CHEMICAL REVIEWS*** 115 (2015) 4744–482.

Superior bio-characteristics of CDs

IN VIVO RENAL EXCRETION

CDs size approx. 2-3 nm (17 kDa) with PEG

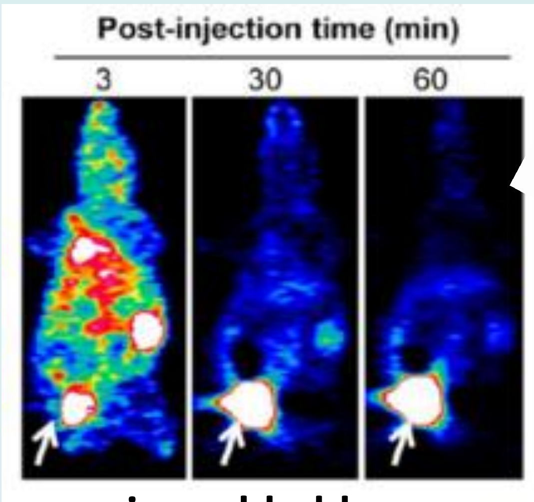

urinary bladder

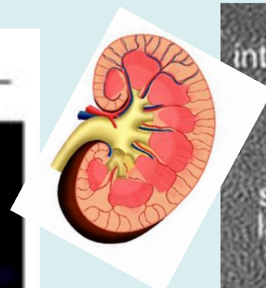

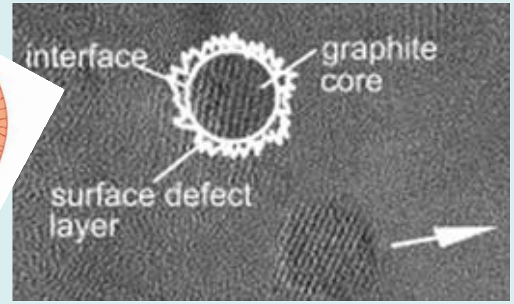

Huang *et al. ACS Nano* **2013**, *7*, 5684.
Nurunnabi et al. *ACS Nano* **2013**, *7*, 6858.

SUPERIOR TUMOR UPTAKE

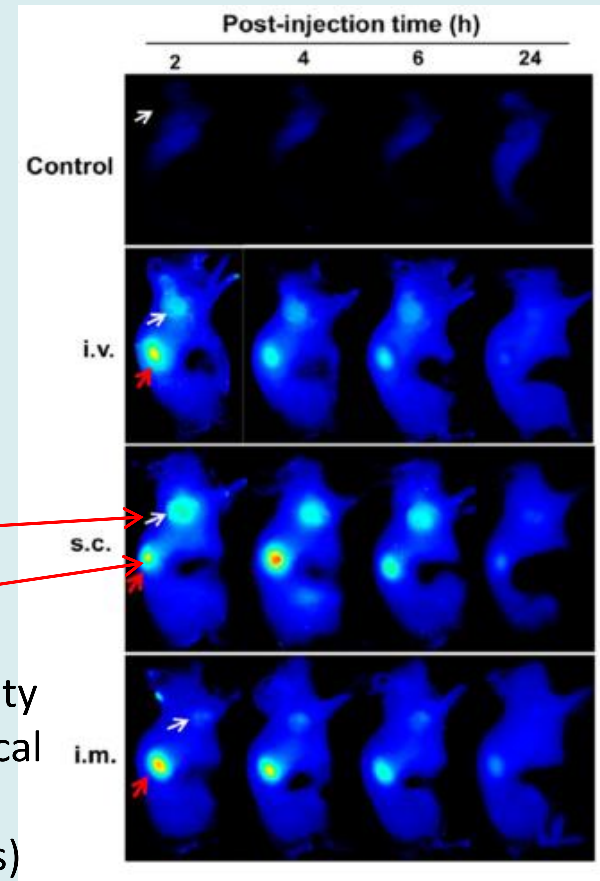

tumor

kidney

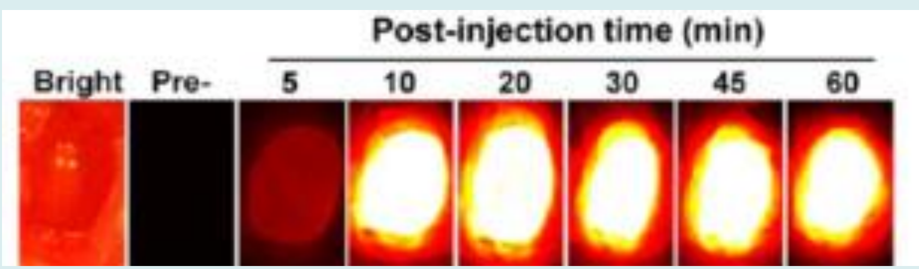

No acute toxicity or morphological changes (10 mg/kg, 22 days)

Blood

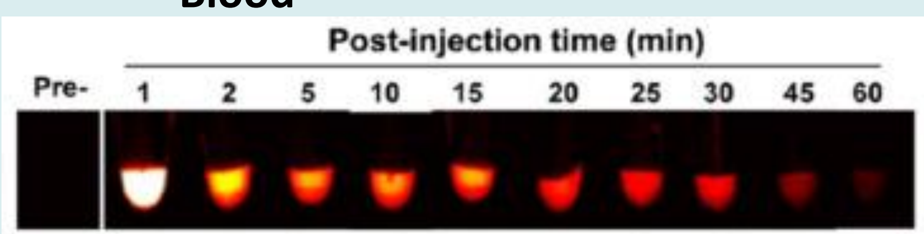

CDs as challenging theranostic agent?

- Photodynamic therapy/targeted drug delivery

Superparamagnetic Iron Oxide (SPIO) NPs in MRI

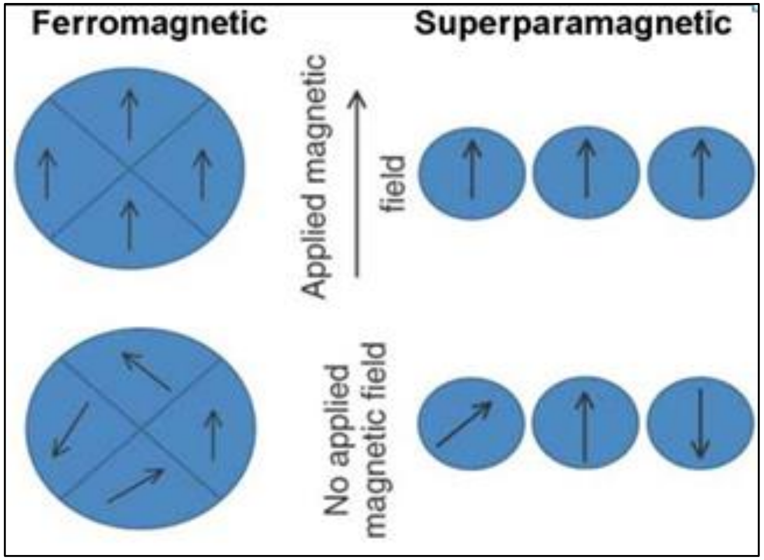

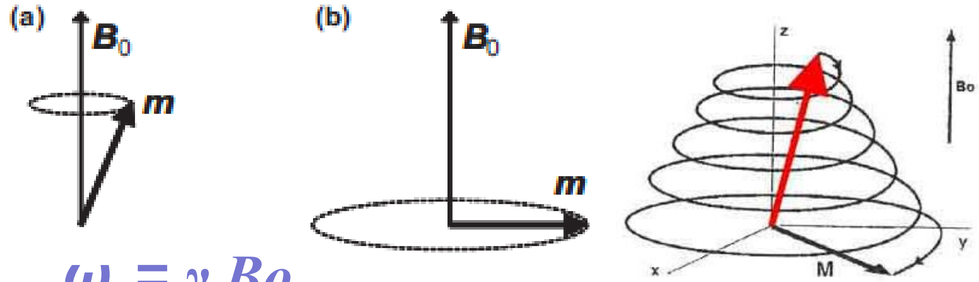

$\omega_L = \gamma . Bo$

- Based on 1H magnetic moments (spin) preceding arround the vector of applied magnetic field (B_0)
- the radio frequency field (B1, MHz, in a pulse sequence) is applied in a plane perpendicular to B_0
- the radio frequency pulse is turned off $\Rightarrow$ the relaxation of the coherent response is measured
- **SPIO shorten T_2 - transverse (or spin–spin) relaxation times $T_2 \Rightarrow$ negative contrast agent**

$$m_z = m(1 - e^{-t/T_1}) \qquad m_{x,y} = m \sin(\omega_0 t + \phi) e^{-t/T_2}$$

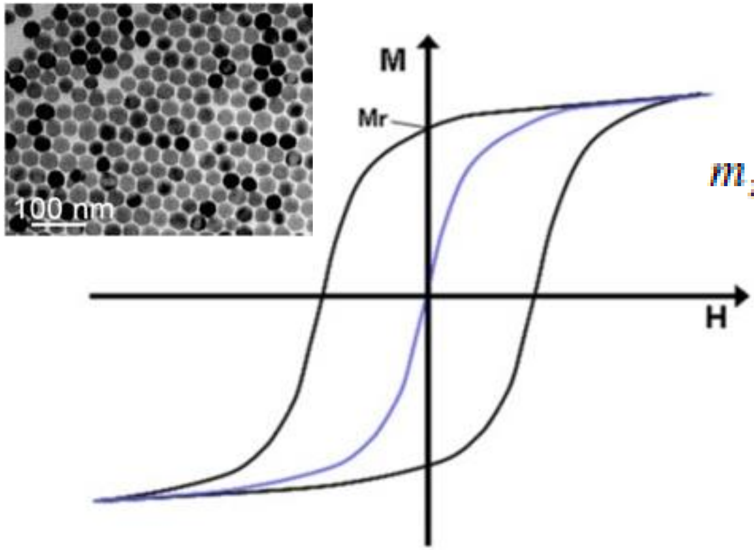

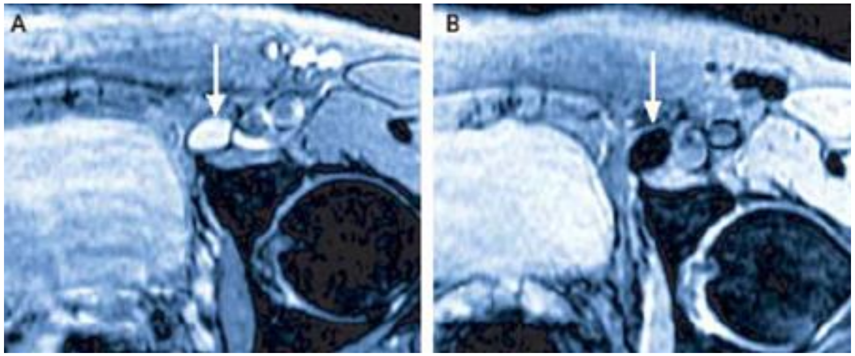

SPIO/bentonite hybrid as per-oral contrast agent in MRI

REGIONAL CENTRE OF ADVANCED TECHNOLOGIES AND MATERIALS
Regionální centrum pokročilých technologií a materiálů

PERORAL MRI AGENT

γ-Fe_2O_3 nanoparticles. One-step thermal decomposition of Fe(II) acetate in air at 400 °C

TEM

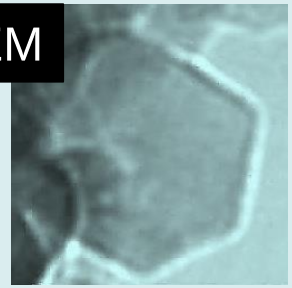

← 20 nm →

SEM

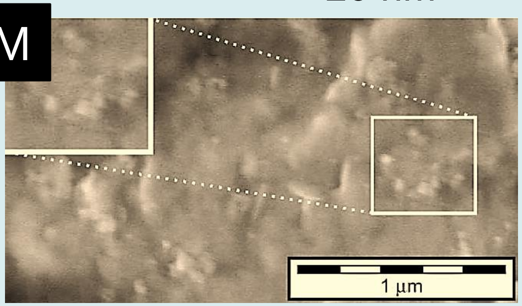

Dispersed in bentonite matrix

Patented product - Peroral MRI negative contrast agent for gastrointestinal tract

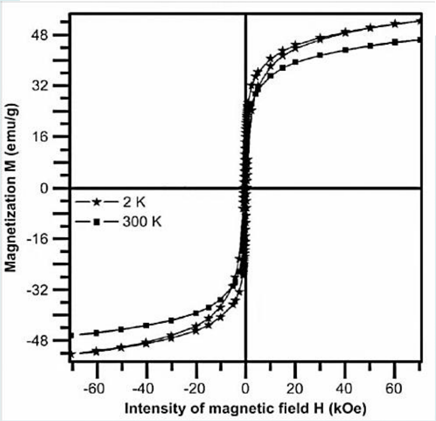

Properties

- Easy to synthesize
- Good magnetic moment 40 emu/g (3T)
- High stability- Low toxicity
- High negative (T_2) MRI contrast

Biomaterials **30, 2855, 2009.**

Lumirem (IT)

SPIO/bent. (Olomouc)

2014-2016

- **Clinical trials** Over 150 patients (FN Olomouc, Banska Bystrica)
- **Negotiation** on the license conditions with Biomedica

Patent No. 300445

SPIO/bentonite hybrid as per-oral contrast agent in MRI

REGIONAL CENTRE OF ADVANCED TECHNOLOGIES AND MATERIALS
Regionální centrum pokročilých technologií a materiálů

EXAMPLES FROM CLINICAL TRIALS

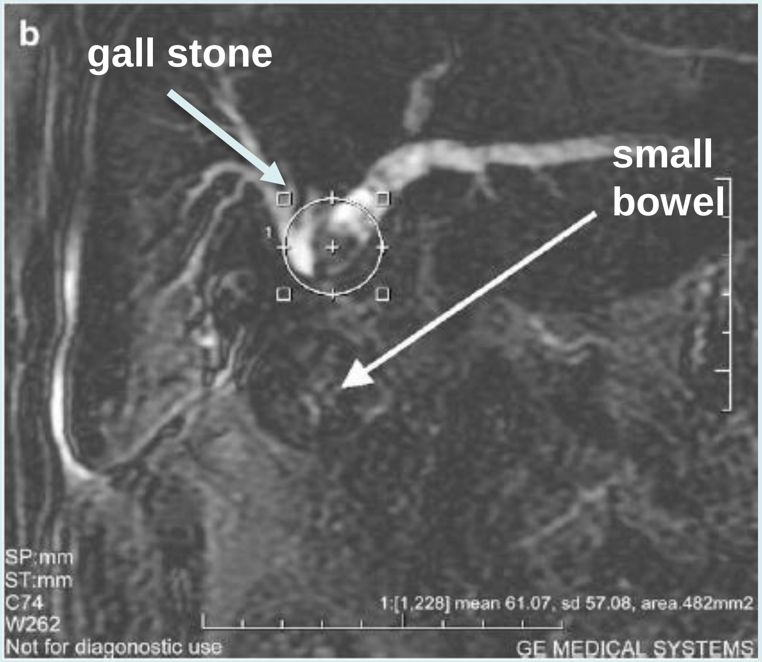

gall stone in a bile duct

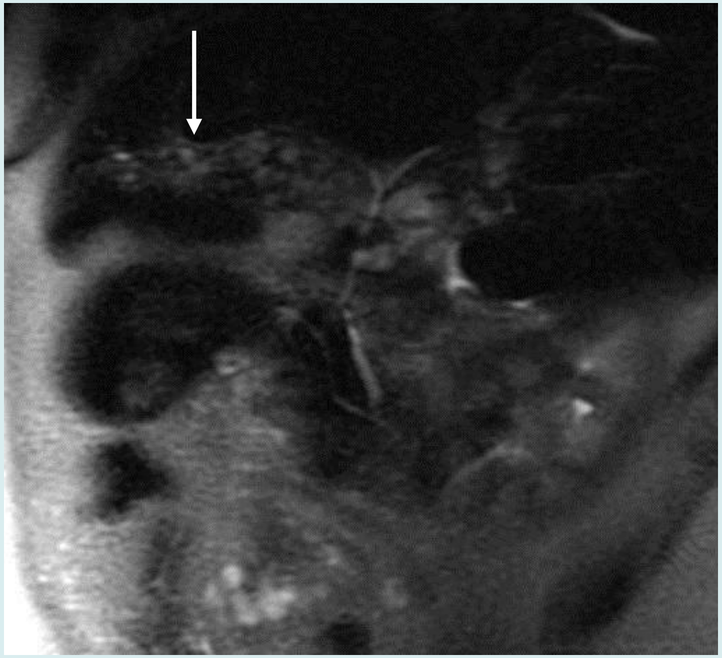

MRCP with the use of negative contrast agent of maghemite/bentonite in small bowel, **numerous extraluminal hyperintense metastases** (arrow)

SPIO/bentonite hybrid as per-oral contrast agent in MRI

REGIONAL CENTRE OF ADVANCED TECHNOLOGIES AND MATERIALS
Regionální centrum pokročilých technologií a materiálů

EXAMPLES FROM CLINICAL TRIALS

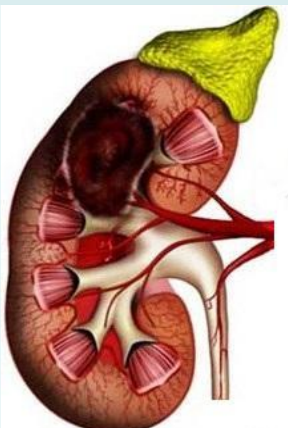

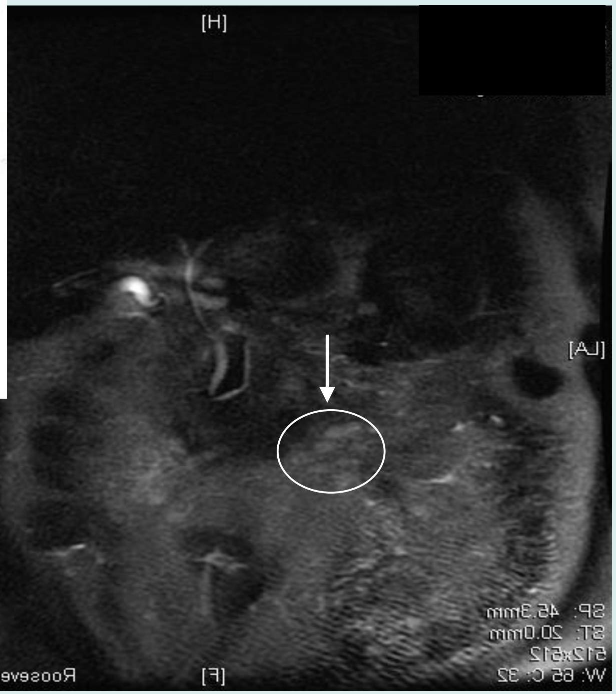

MRCP with experimental oral contrast agent, 65y. man, unknown **Grawitz tumor** of the right kidney, multiple metastases intraperitoneal paraluminal (arrow)

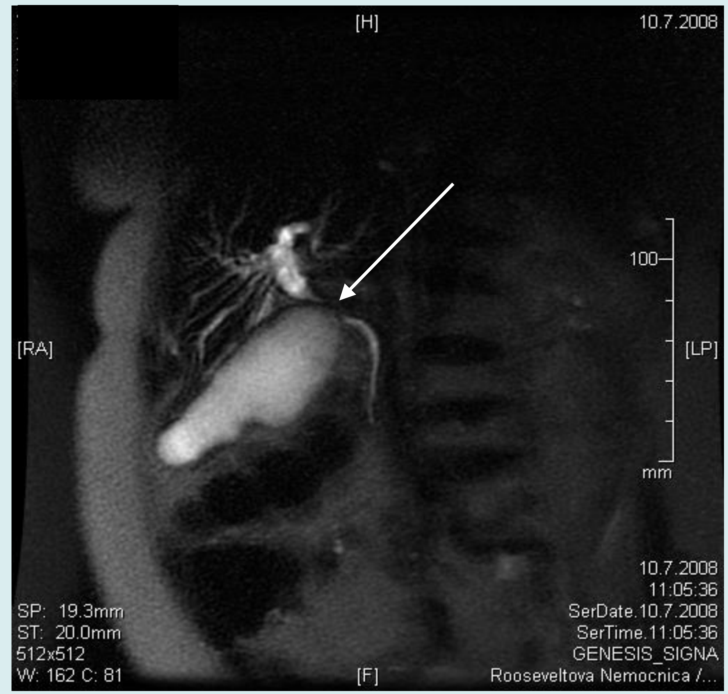

88 y. woman - **malignant stenosis of bile duct**

SPIO in Targeted Drug Delivery and Magnetic Theranostics

Various architectures of magnetic hybrid nano-assemblies, ascribing different attributes to the final theranostics.

Key requirements:

- Nano-assemblies facilitating very high structural and colloidal stability and stability in the blood environment
- Minimum non-specific interactions.
- Appropriate drug loading and controlled release kinetics.
- Hydrodynamic size smaller than 200 nm.
- Magnetic crystallites close to superparamagnetic limits for maximum magnetic properties and MRI imaging
- Produced through high yield processes.
- Relatively cost effective process.

CHEMICAL REVIEWS

Review

pubs.acs.org/CR

Targeted Drug Delivery with Polymers and Magnetic Nanoparticles: Covalent and Noncovalent Approaches, Release Control, and Clinical Studies

Karel Ulbrich,[†,§] Kateřina Holá,[‡,§] Vladimir Šubr,[†] Aristides Bakandritsos,[‡] Jiří Tuček,[‡] and Radek Zbořil[*,‡]

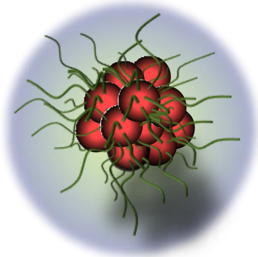

SPIO based theranostics in RCPTM with condensed nanoclusters „coNCs“

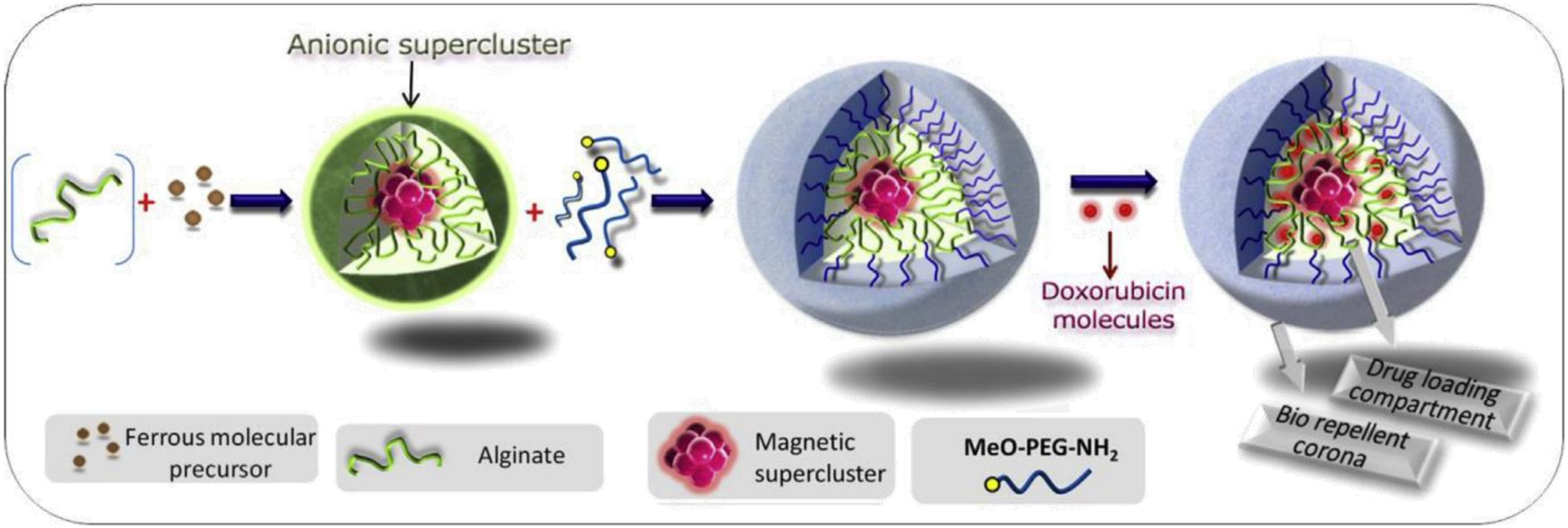

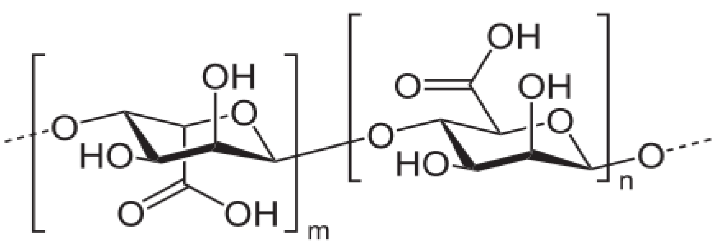

Alginic Acid biopolymer

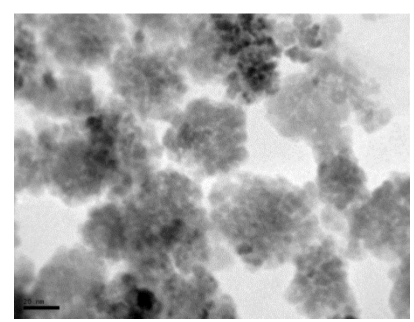

~25 SPIONs/cluster

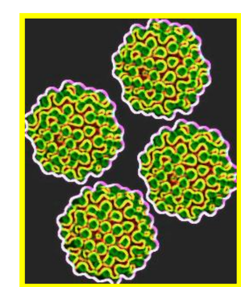

A. Bakandritsos et al *Small*, **2012**, 8, 2381–2393.

G. Zoppellaro et al. *Chem. Mater.*, 2014, **26**, 2062–2074.

Y. Sarigiannis, et al. *Biomaterials*, **2016**, 91, 128–139.

coNCs theranostics - superior magnetic characteristics

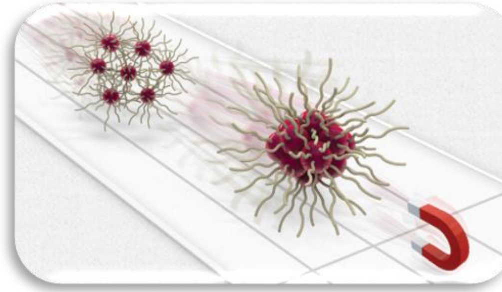

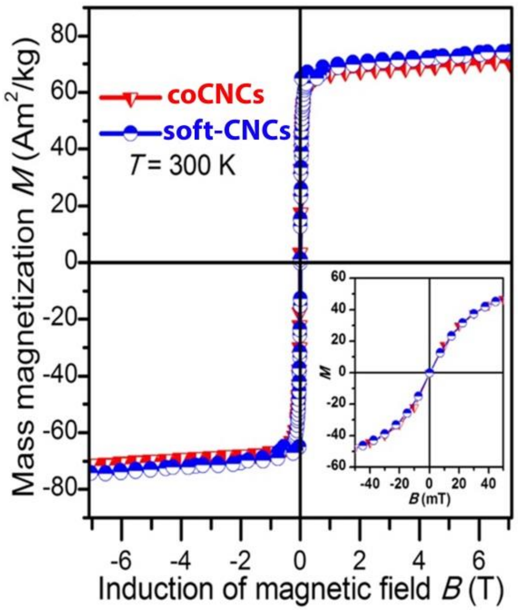

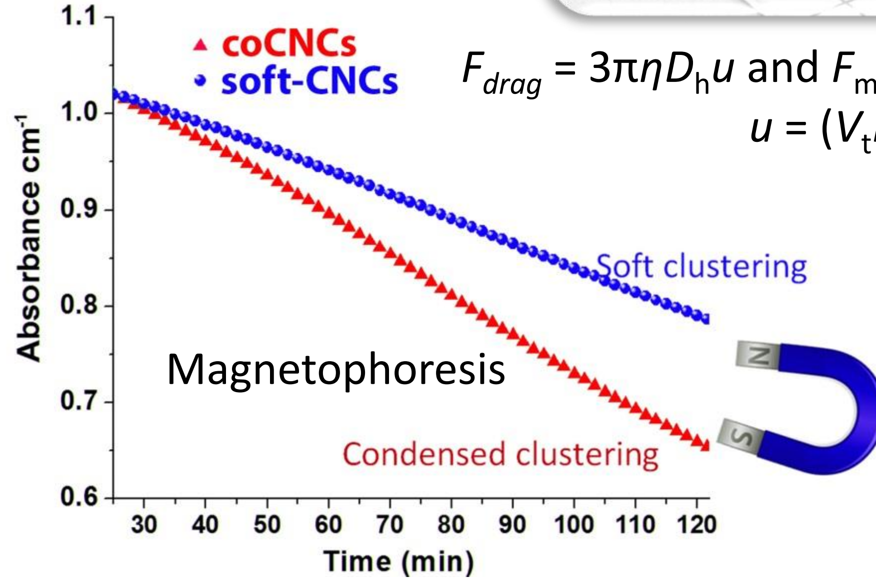

$F_{drag} = 3\pi\eta D_h u$ and $F_{mag} = (V_t M_s \nabla)\boldsymbol{B}$

$u = (V_t M_s \nabla)\boldsymbol{B}/3\eta\pi D_h$

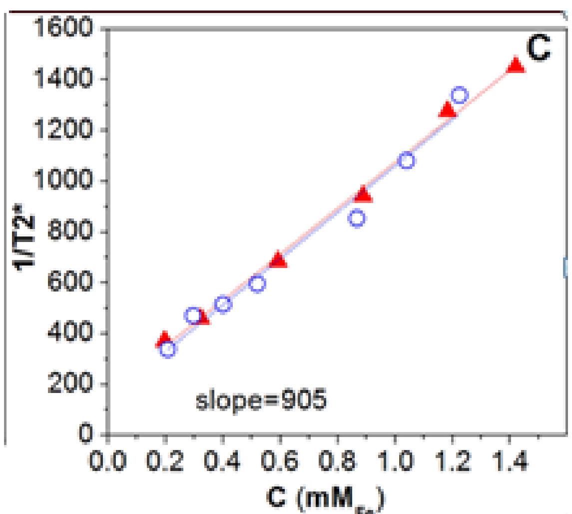

- **higher magnetophoretic response** compared to softNCs $\Rightarrow$ **better manipulation with EMF**
- High saturation magnetization, **still perfect SP behavior**
  - coNCs display large transverse relaxivities $\Rightarrow$ top relaxivity considering the size of assembly $\Rightarrow$ **excellent MRI properties**
    - r2= 400 s-1 mM-1Fe
    - r2*= 900 s-1 mM-1Fe

coNCs theranostics - superior bio-characteristics

High drug loading (15%wt) and excellent colloidal stability after PEGylation (both in physiological solution and in human blood plasma)

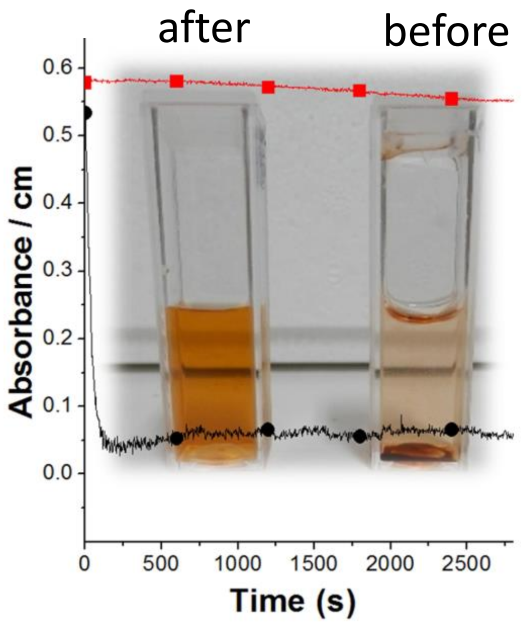

AMF ttriggered drug release

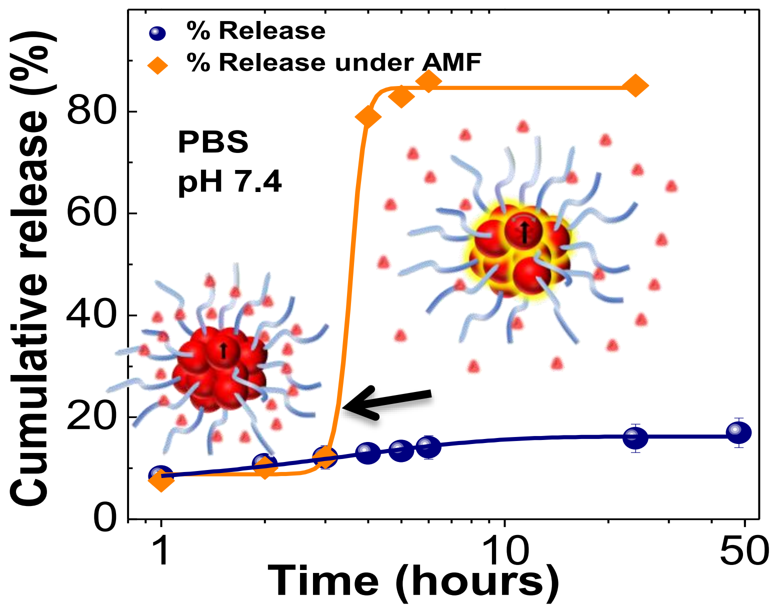

Prevention of non-specific cell-particle interactions (cell uptake) due to secondary PEGylation

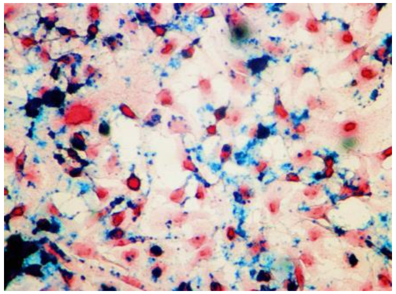

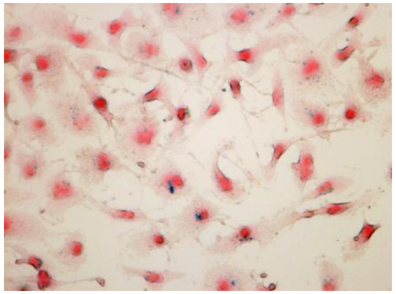

Improved biodistribution due to PEGylation and hydrodynamic diameter below 100 nm:

SPIO is not concentrated in the liver ⇒ better targeting to the cancer

coNCs theranostics – in vivo imaging/targeting breast cancer; passive versus active targeting

In vivo imaging through Multispectral Optoacoustic Tomography, based on absorbance of the magnetic cores solely within the NIR transparent spectral window of the tissue.

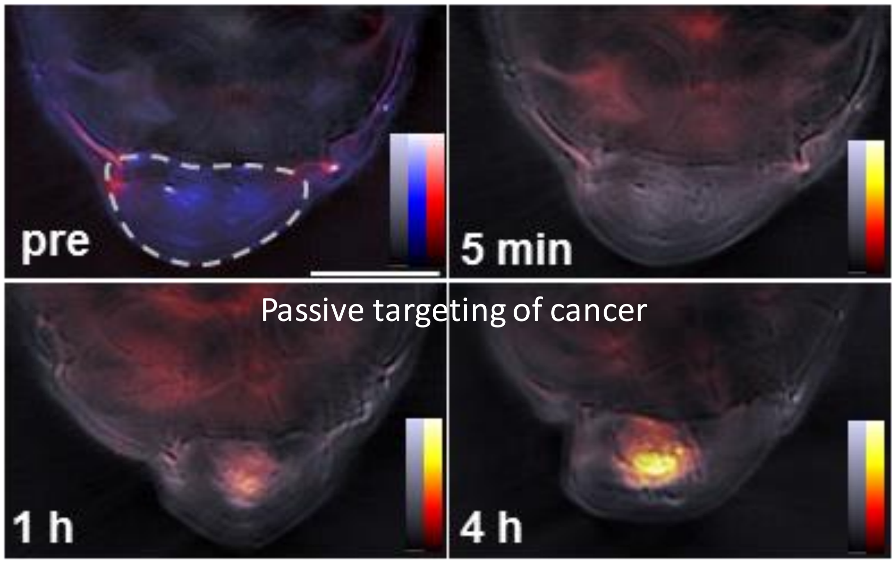

coNCs **passively target** the tumor area (4T1 xenografts), after tail vein intravenous administration due to EPR effect.

Notes: Magnetic species – yellow color
Deoxygenated blood – blue
(hypoxic conditions in tumor tissue)
Oxygenated blood - red

Y. Sarigiannis et al. *Biomaterials*, **2016**, 91, 128–139.

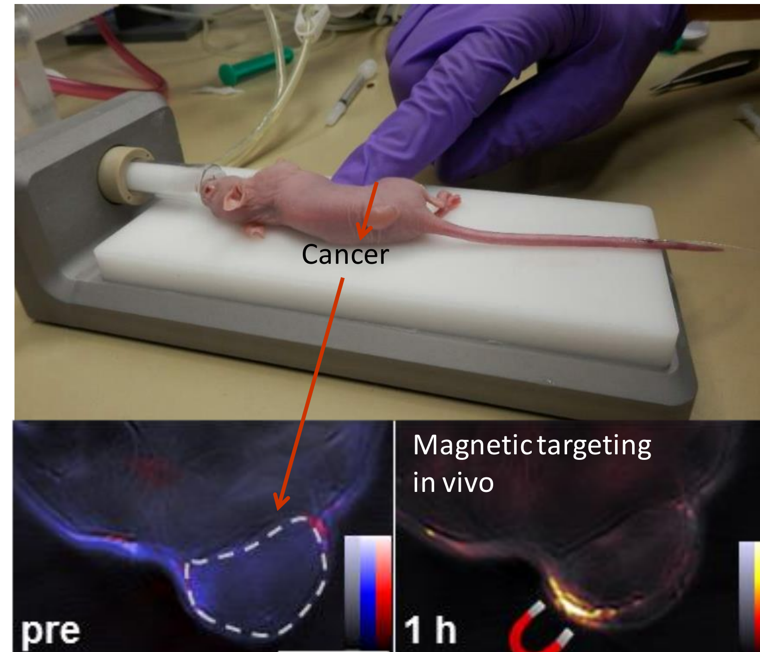

Active targeting - Theranostic agent responds very effectively to EMF ⇒ all detected particles are concentrated at the nursing vessel of the tumour after their tail injection - the local concentration of the drug is higher and able to reach normally unreachable areas of the tumourous tissue

REGIONAL CENTRE OF ADVANCED TECHNOLOGIES AND MATERIALS
Regionální centrum pokročilých technologií a materiálů

Thanks for your attention!

All colleagues from RCPTM

M. Kolář, M. Heřman
Antimicrobial testing, MRI

J. Konvalinka, P. Cígler
Carbon dots, nanodiamonds

A. Bakandritsos
Targeted drug delivery

F. Besenbacher, M. Dong
Interactions with 2D

P. Carretta, A. Lascialfari
MRI - theory

V. Georgakilas, D. Petridis
Graphene functionalization

R. Varma
Toxicity of NPs, nanocatalysis

F. Vianello
Biosensors

A. Rogach
Hybrids with quantum dots

AB Bourlinos, M. Karakassides
Carbon hybrids

EP. Giannelis, M. Krysman,
Carbon dots

S. Ohkoshi
Magnetic nanoparticles

A. Gedanken
Antimicrobial NPs

R. Stollberger, C. Divoki
MRI-applications

New chalenges in nanomedicine – quantum dots?

QDs - nanocrystals of semiconductor materials, such as CdSe, CdTe, in which electron-hole pairs can be created and confined. When the QDs are exposed to light, electron-hole pairs are excited and fluoresce. The frequency of emitted light increases as the size of the quantum dot decreases ⇒ **tunable PL**

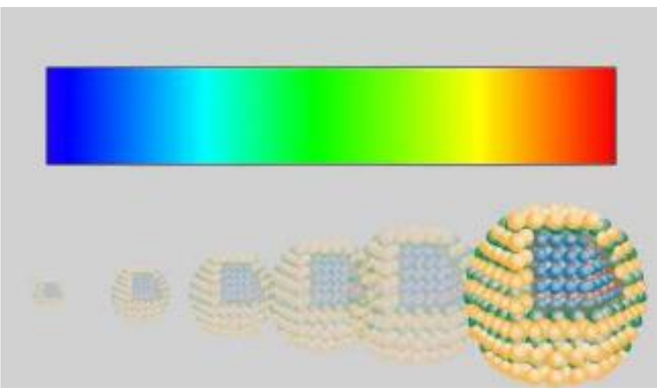

Bioimaging

Photodynamic/ photothermal therapy

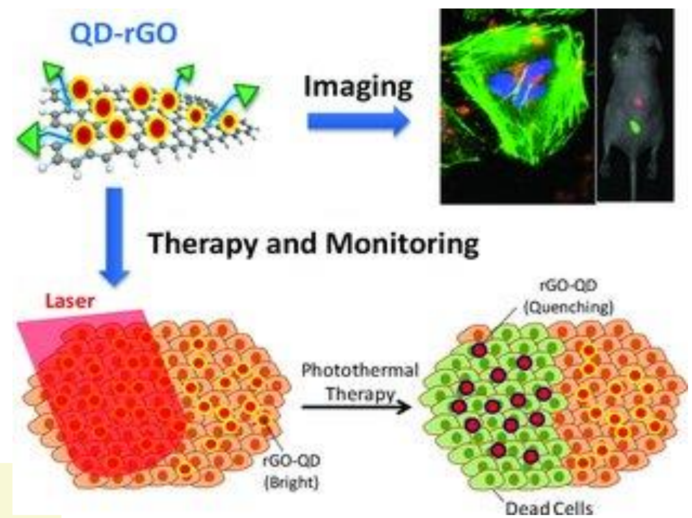

Drug delivery

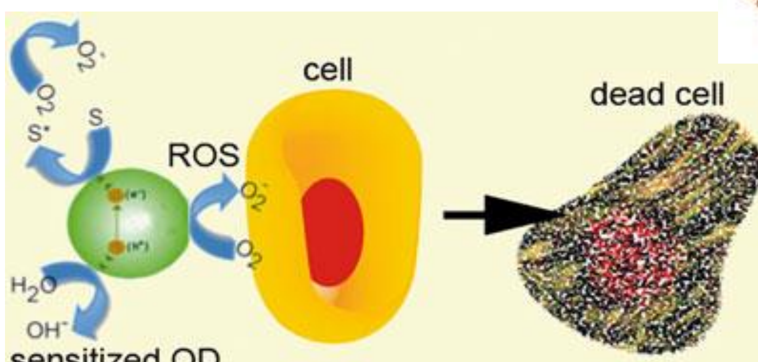

Problems:

- Biodistribution
- Toxicity (heavy metals)

Targeted drug delivery – EPR passive targeting

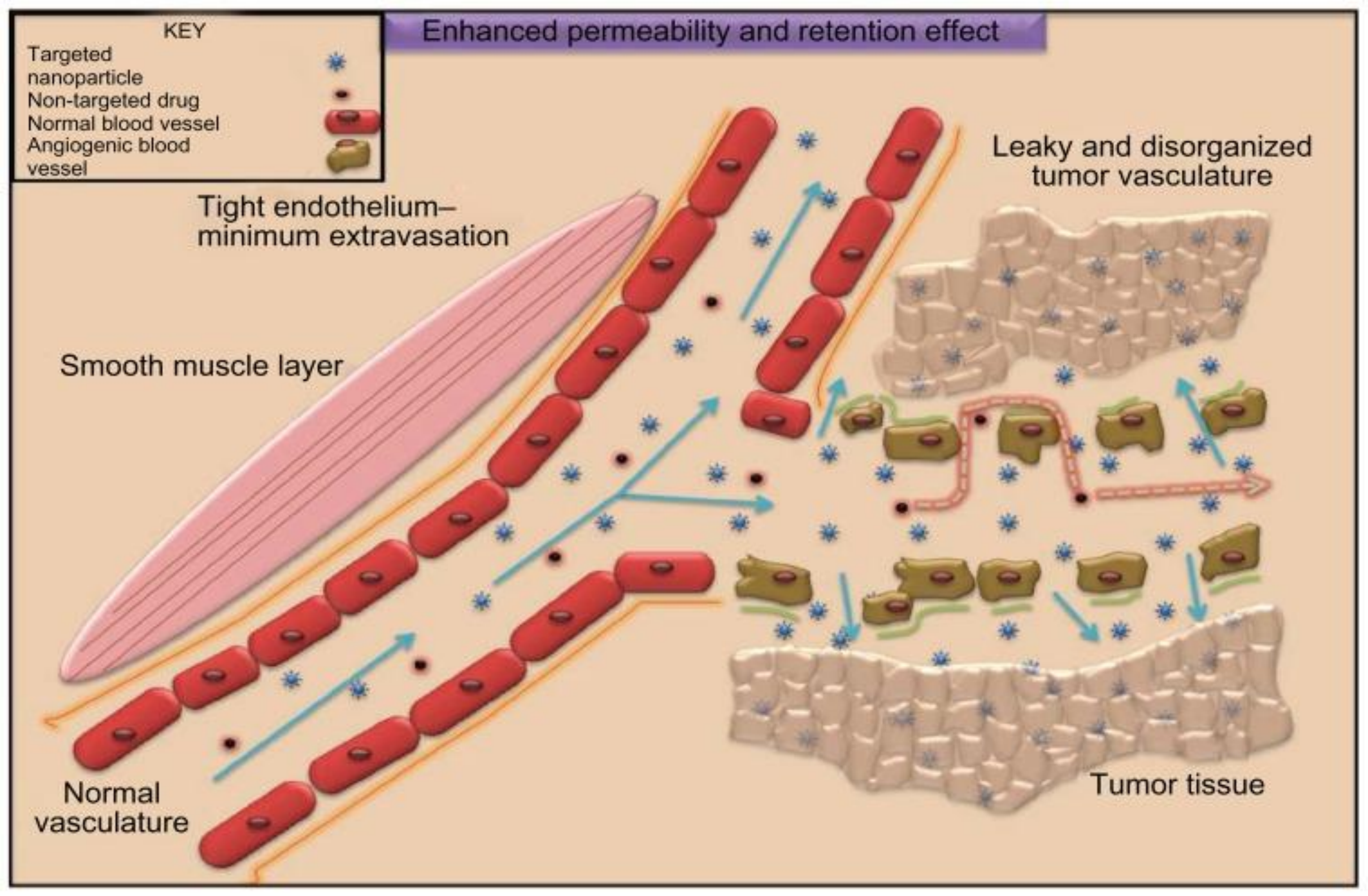

EPR effect operating in tumor milieu permitting accumulation of NPs in cancer cells. Blood vessels in tumor tissue have defective architecture with gaps as large as 200–1000 nm allowing NPs to extravasate and accumulate inside the tumor tissue. The retention time of drugs packed in nanoparticles is ten times higher than that of unpacked

Carbon dots - Challenges

Drug delivery

- C-dots + PEG
- Doxorubicin loading + pH release
- FRET (Fluorescence Resonance Energy Transfer) monitoring of drug release

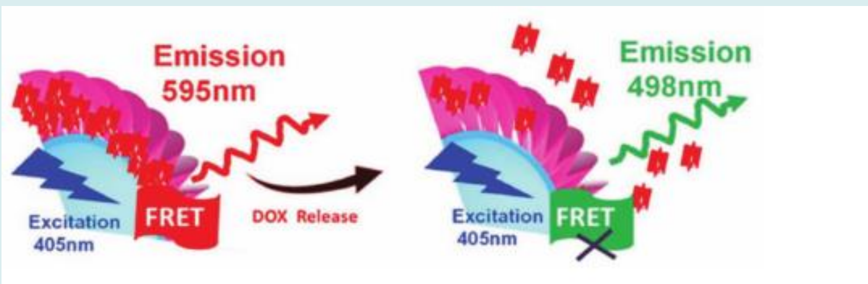

Thermodynamic therapy - ROS generation

- under irradiation by blue/green lamp: ROS generation
- no toxicity for normal cells

Red emission, selective labeling of cell nucleus/ cytoplasm; superior uptake by cancer cells – effect of surface charge

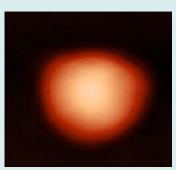

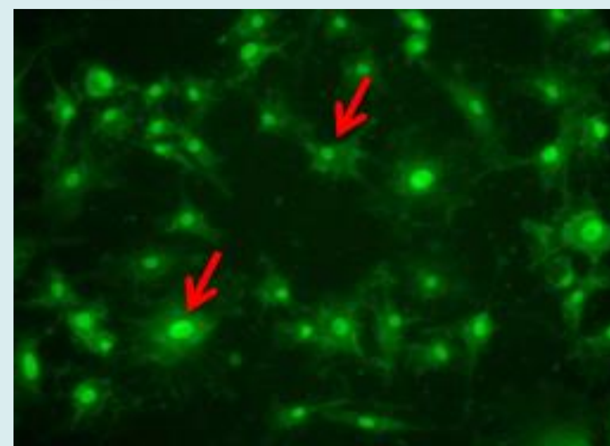

mouse fibroblast NIH/3T3 cells labeled with CDs

Bourlinos te al. Chem. Mater 24 (2012) 6.

Tang. et al. *Adv. Mater.* **2013**, *25*, 6569–6574.

Markovic, *et al. Biomaterials* **2012**, *33*, 7084–7092.

Christensen, et al. *J. Biomed. Nanotechnol.* **2011**, *7*, 667–676.

In vitro optoacoustic studies were performed in a tissue mimicking phantom obtained using cylindrical phantoms of 2 cm diameter. They were prepared using a gel made from distilled water, containing Agar (Sigma-Aldrich) for jellification (1.3% w/w) and an intralipid 20% emulsion (Sigma-Aldrich) for light diffusion (6% v/v), resulting in a gel presenting a reduced scattering coefficient of m's z 10 cm1 and no specific absorbance as to allow precise estimation of light energy deposition. A 3 mm diameter straw, transparent for near infra-red light and ultrasound waves, was filed with the sample solution and included close to the center of the tissue mimicking phantom, alongside with a similar straw filed with India Black Ink (OD: 0.3) as a reference. MSOT acquisition was then performed using illumination wavelengths in 5 nm steps

between 680 and 900 nm for the spectral experiments.

Animal experiments: All animal experiments were performed in accordance to the institutional guidelines and approved by the government of Upper Bavaria (Germany). A xenograft tumour model was employed using 4T1 murine breast cancer cells. 8 weeks old adult female athymic nude-Foxn1 nude mice (Harlan, Germany) were inoculated subcutaneously in the middle of the back in the region for the upper pelvis with 1,5.106 4T1 (CRL-2539) cells in 50 mL PBS. Animals were imaged in the MSOT system once the tumour reached a size of 8 mm diameter. Acquisition was performed using 20 averages per position in 1 mm steps throughout the tumour using 680, 710, 740, 770, 800, 830, 860 and 890 nm as illumination wavelengths, at different time points after injection of the nanoparticles (before, 5 min, 1 h and 4 h after injection). When the use of a magnet was required, a cylindrical Nd-Fe-B magnet (dimensions: diameter ¼ 20 mm, thickness ¼ 10 mm) was used and applied directly on the tumor during injection. During image acquisition, the magnet was removed.